HHS Public Access

Author manuscript

Pediatr Radiol. Author manuscript; available in PMC 2015 June 01.

Published in final edited form as:

Pediatr Radiol. 2015 June ; 45(6): 804–813. doi:10.1007/s00247-014-3246-z.

4-D flow magnetic resonance imaging: blood flow quantification compared to 2-D phase-contrast magnetic resonance imaging and Doppler echocardiography

Maya Gabbour,
Department of Medical Imaging #9, Ann & Robert H. Lurie Children's Hospital of Chicago, 225 E. Chicago Ave., Chicago, IL 60611, USA

Susanne Schnell,
Department of Radiology, Northwestern University Feinberg School of Medicine, Chicago, IL, USA

Kelly Jarvis,
Department of Biomedical Engineering, McCormick School of Engineering, Northwestern University, Evanston, IL, USA

Joshua D. Robinson,
Department of Pediatrics, Division of Pediatric Cardiology, Ann & Robert H. Lurie Children's Hospital of Chicago, Chicago, IL, USA. Department of Pediatrics, Northwestern University Feinberg School of Medicine, Chicago, IL, USA

Michael Markl, and
Department of Radiology, Northwestern University Feinberg School of Medicine, Chicago, IL, USA. Department of Biomedical Engineering, McCormick School of Engineering, Northwestern University, Evanston, IL, USA

Cynthia K. Rigsby
Department of Medical Imaging #9, Ann & Robert H. Lurie Children's Hospital of Chicago, 225 E. Chicago Ave., Chicago, IL 60611, USA. Department of Radiology, Northwestern University Feinberg School of Medicine, Chicago, IL, USA

Cynthia K. Rigsby: crigsby@luriechildrens.org

Abstract

Background—Doppler echocardiography (echo) is the reference standard for blood flow velocity analysis, and two-dimensional (2-D) phase-contrast magnetic resonance imaging (MRI) is considered the reference standard for quantitative blood flow assessment. However, both clinical standard-of-care techniques are limited by 2-D acquisitions and single-direction velocity encoding and may make them inadequate to assess the complex three-dimensional hemodynamics seen in

Correspondence to: Cynthia K. Rigsby, crigsby@luriechildrens.org.

Conflicts of interest None

congenital heart disease. Four-dimensional flow MRI (4-D flow) enables qualitative and quantitative analysis of complex blood flow in the heart and great arteries.

Objectives—The objectives of this study are to compare 4-D flow with 2-D phase-contrast MRI for quantification of aortic and pulmonary flow and to evaluate the advantage of 4-D flow-based volumetric flow analysis compared to 2-D phase-contrast MRI and echo for peak velocity assessment in children and young adults.

Materials and methods—Two-dimensional phase-contrast MRI of the aortic root, main pulmonary artery (MPA), and right and left pulmonary arteries (RPA, LPA) and 4-D flow with volumetric coverage of the aorta and pulmonary arteries were performed in 50 patients (mean age: 13.1±6.4 years). Four-dimensional flow analyses included calculation of net flow and regurgitant fraction with 4-D flow analysis planes similarly positioned to 2-D planes. In addition, 4-D flow volumetric assessment of aortic root/ascending aorta and MPA peak velocities was performed and compared to 2-D phase-contrast MRI and echo.

Results—Excellent correlation and agreement were found between 2-D phase-contrast MRI and 4-D flow for net flow (r=0.97, P<0.001) and excellent correlation with good agreement was found for regurgitant fraction (r= 0.88, P<0.001) in all vessels. Two-dimensional phase-contrast MRI significantly underestimated aortic (P= 0.032) and MPA (P<0.001) peak velocities compared to echo, while volumetric 4-D flow analysis resulted in higher (aortic: P=0.001) or similar (MPA: P=0.98) peak velocities relative to echo.

Conclusion—Excellent flow parameter agreement between 2-D phase-contrast MRI and 4-D flow and the improved volumetric 4-D flow velocity analysis relative to echo suggests that 4-D flow has the potential to become a clinical alternative to 2-D phase-contrast MRI.

Keywords

Cardiovascular magnetic resonance; 4-D flow; Phase-contrast; Magnetic resonance imaging; Pediatric; Congenital heart disease

Introduction

Doppler echocardiography (echo) is the gold standard modality for blood flow velocity assessment. Two-dimensional (2-D) phase-contrast MRI provides better access to all vascular segments and is considered the standard for quantifying blood flow [1–7]. Clinical standard-of-care echocardiography and standard 2-D phase-contrast MRI acquire data with only single-direction velocity encoding, in line with the beam trajectory for echo and perpendicular to the slice orientation for 2-D phase-contrast MRI, and are additionally limited by velocity analysis in a single 2-D plane. Although both methods are considered reference standards, their inherent limitations may make them inadequate to characterize the complex 3-D hemodynamics seen in congenital heart disease.

Cardiac and respiratory-gated time-resolved four-dimensional flow MRI (4-D flow) enables blood flow measurement in three spatial directions with full heart and great artery volumetric coverage. Retrospective data analysis allows for flow quantification at any selected region of interest. Methodological advances including improved respiratory gating

and parallel imaging allow for thoracic 4-D flow data acquisition in 8–15 min and have made 3-D blood flow assessment feasible [8–12]. Previous studies have reported the application of 4-D flow in patients with bicuspid aortic valve, aortic coarctation, tetralogy of Fallot, Fontan circulation and transposition of the great arteries [13–20]. These studies have shown the potential for 4-D flow to improve characterization of complex flow hemodynamics seen in congenital heart disease. Studies have also shown good correlation between 2-D phase-contrast MRI and 4-D flow parameters and the ability of 4-D flow to improve peak velocity quantification because of its full volumetric coverage [21–24]. In addition, studies have demonstrated low observer variability and good test-retest reliability for the quantification of hemodynamic parameters (flow, peak velocity) from 4-D flow MRI data [25–28]. Limitations of prior studies include small subject numbers, limited analysis of flow quantification in children, and limited comparison of peak velocities to echo. It was therefore the purpose of this study to compare 4-D flow quantification of aortic and pulmonary flow parameters to the reference standards 2-D phase-contrast MRI and echo in a large cohort of children and young adults.

Materials and methods

We obtained consent to perform 4-D flow following a clinically indicated cardiac MRI study per a prospective protocol that was approved by our institutional review board and compliant with the Health Insurance Portability and Accountability Act.

Study cohort

We queried institutional PACS and MRI databases for children and young adults who underwent clinically indicated cardiac MRI including 2-D phase-contrast MRI and 4-D flow during the same examination. From December 2011 through November 2012, 50 subjects were identified (age range 3.9–29.0 years; mean age: 13.1±6.4 years). Echo data were available for 39 of the 50 patients.

Magnetic resonance imaging

Imaging was performed on a 1.5-tesla scanner (MAGNETOM Avanto or Aera; Siemens Healthcare USA, Malvern, PA) with high-performance gradient subsystems (45 mT/m maximum amplitude; 200 mT/m/ms maximum slew rate). A 6-channel matrix coil was used for imaging on the Avanto and a 16-channel matrix coil was used for imaging on the Aera. Two-dimensional phase-contrast MRI and 4-D flow were obtained after gadofosveset trisodium contrast administration (0.12 ml/kg Ablavar®; Lantheus Medical Imaging, North Billerica, MA) as per the magnetic resonance angiography (MR angiography) portion of the clinical protocol in all patients. Ablavar® is the standard contrast agent used for clinical cardiovascular MR angiography examinations at our institution if the examination is not specifically directed toward assessment of late gadolinium enhancement. Ablavar® is given prior to the 2-D phase-contrast MRI and 4-D flow sequences to improve the signal-to-noise ratio of these images [29]. General anesthesia was utilized per standard clinical protocol. Small-field-of-view cardiac shimming was performed at the vessel of interest. Two-dimensional phase-contrast MRI and 4-D flow were performed at magnet isocenter with the patient free-breathing.

Two-dimensional phase-contrast magnetic resonance imaging

Two-dimensional phase-contrast MRI sequences included flow assessment in one or any combination of the following vessels per the clinical protocol indication: aortic root, main pulmonary artery (MPA), right pulmonary artery (RPA), and left pulmonary artery (LPA). Clinical standard-of-care 2-D phase-contrast MRI was acquired with single-direction (through-plane) velocity encoding. The 2-D phase-contrast MRI aortic root imaging plane was positioned perpendicular to the long axis of the aortic lumen at the aortic valve leaflet tips during systole. The 2-D phase-contrast MRI main pulmonary artery plane was positioned perpendicular to the long axis of the MPA distal to the pulmonary valve in systole. RPA and LPA 2-D phase-contrast MRI sequences were performed when flow analysis through each of the branch pulmonary arteries was clinically indicated. Two-dimensional phase-contrast MRI planes were placed perpendicular to the long axes of each branch pulmonary artery. Two-dimensional phase-contrast MRI imaging parameters are listed in Table 1. Velocity encoding for each vessel was chosen based on echocardiography velocity for each vessel. If aliasing was present on any acquisition, the acquisition was repeated with a higher velocity encoding.

Two-dimensional phase-contrast MRI data were analyzed using Medis QFLOW (Medis Medical Imaging Systems, Leiden, The Netherlands). Vessel contours were adjusted manually to account for vessel motion. Net flow (ml/cycle), regurgitant fraction (%), and peak velocity (m/s) were recorded.

Four-dimensional flow

Four-dimensional flow was performed using a time-resolved 3-D phase-contrast gradient echo sequence with three-directional velocity encoding. If the clinically indicated MRI examination was tailored to the aorta only, the 4-D flow sequence was acquired in the oblique sagittal plane. For an examination tailored to the aorta, pulmonary arteries, and pulmonary or systemic veins, 4-D flow data were acquired using an imaging volume to include all major thoracic vessels (Fig. 1). To minimize breathing artifacts, the 4-D flow acquisition was respiratory-gated using adaptive diaphragm navigator gating with variable efficiency using a fixed acceptance window [30]. Acquired data were phase-encoded in k_y–k_z-space according to position in the respiratory cycle. Data acquired closer to end-expiration (maximum diaphragmatic position), at which time the chest shows the least motion, were assigned to central k-space. Data closer to inspiration (minimum diaphragmatic position) were assigned to outer k-space positions. This approach mitigates respiration artifacts and allows for larger navigator efficiencies (75–90%) compared to traditional navigator gating techniques (40–50%). The 4-D flow velocity encoding was set slightly below the maximum velocity value obtained by 2-D phase-contrast MRI in all vessels included in the 4-D flow field-of-view so that there would be maximum signal in the entire volume of interest for 4-D flow analysis. Anti-aliasing pre-processing was performed on all 4-D flow datasets to eliminate any aliasing caused by the slightly lower velocity encoding values chosen for 4-D flow relative to 2-D phase-contrast MRI. Four-dimensional flow was performed in 47 of the 50 children and young adults with a parallel imaging acceleration factor of 2. The use of k-t GRAPPA (spatially and temporally accelerated GeneRalized Autocalibrating Partially Parallel Acquisition) acceleration became available

for 3 of the 50 patients with an acceleration factor of 5 utilized to shorten scan times while maintaining a similar temporal resolution. The 4-D flow in-plane spatial resolution was adjusted to acquire four voxels of data across the diameter of each vessel of interest. An in-plane resolution of 4.1×2.5 mm was the minimal resolution utilized only in two teenage patients with larger great arteries. Four-dimensional flow acquisition parameters are listed in Table 1.

Four-dimensional flow data post-processing was performed by a single operator (M.G.), who was blinded to the quantitative 2-D phase-contrast MRI results. Four-dimensional flow data processing included corrections for concomitant gradient fields, eddy currents and velocity aliasing, as previously described [6, 31]. The method used for eddy current correction was based on the technique originally developed by Walker et al. [31] and uses thresholding to identify regions with static tissue (the static tissue is separated from regions with blood flow and noise using the standard deviation of the pixel's velocity time course). These regions are then used to estimate eddy-current-induced linearly varying phase-offset errors, which are subsequently subtracted from the entire image. Open-source tools programmed in MATLAB (MathWorks, Natick, MA) were used for noise masking and subsequent calculation of a time-averaged 3-D phase-contrast MR angiography dataset (Fig. 1) similar to methods reported by Bock et al. [32]. Next, the data were loaded into commercial visualization software (EnSight 9.2; CEI, Apex, NC) and 2-D analysis planes were carefully placed at the similar anatomical positions used for 2-D phase-contrast MRI for each vessel (Fig. 1) using anatomical landmarks on the 3-D phase-contrast MR angiogram and anatomical images to position the planes similarly. For each analysis plane, the 3-D phase-contrast MR angiographic vessel geometry was used to define vessel lumen contours to automatically calculate net flow (ml/cycle) and regurgitant fraction (%) [12]. To take advantage of the full volumetric coverage provided by 4-D flow, peak systolic velocities were determined inside cylindrical volumes positioned to cover the entire aortic root and ascending aorta and MPA (Fig. 1). The cylinder method avoids inclusion of areas close to the vessel wall and adjacent vascular structures, thereby avoiding artifacts. To extract volumetric peak flow velocities, we queried all voxels inside the aortic root and ascending aorta and MPA volumes to identify the voxel with the highest absolute velocities within the entire volume and over the cardiac cycle. We did not record total time taken to post-process a 4-D flow dataset; this time varied by the complexity of the case. For an individual fully trained in 4-D flow post-processing, the time taken to post-process a 4-D flow dataset focused on the aorta was approximately 30 min. The time taken to post-process a complex 4-D flow dataset, such as a Fontan dataset, was approximately 1.5 h.

Echocardiography

Clinically indicated echo studies were performed on Philips IE33 ultrasound machines (Philips Healthcare, Best, The Netherlands) using the optimal transducer for patient size with single-direction velocity encoding. A single pediatric cardiologist (J.D.R.) observer retrospectively reviewed the echo images. The highest velocity obtained by continuous wave Doppler, from the apical or suprasternal window for the aorta and from the subcostal or parasternal short-axis plane for the MPA, was recorded for comparison with 2-D phase-contrast MRI and 4-D flow.

Statistical analysis

All continuous values are reported as mean±standard deviation. To compare net flow, regurgitant fraction, and peak velocity between 2-D phase-contrast MRI and 4-D flow, and to compare peak velocity between 2-D phase-contrast MRI and echo, we performed two-sided paired *t*-tests. Differences were considered significant for $P<0.05$. To identify the correlation between different modalities for net flow, regurgitant fraction and peak velocity, we performed linear regression and calculated the Pearson correlation coefficient r; a correlation was considered significant for $P<0.05$. To identify the agreement among the different modalities for net flow, regurgitant fraction and peak velocity, we generated Bland-Altman plots and calculated the mean difference and limits of agreement (±1.96 standard deviation [SD]). All statistical analysis was performed using MATLAB (MathWorks, Natick, MA).

Results

Patient demographics are summarized in Table 2. Two-dimensional phase-contrast MRI was clinically indicated, completed and analyzed at the time of the clinical examination for the aortic root in 50 patients, for the MPA in 41 patients, and for the RPA and LPA in 30 patients. Four-dimensional flow was successfully completed and analyzed in all 50 patients. Echo data were available for 39 patients who had an echo examination within 3.15±4.0 months of the MRI. Thirty-five of these patients had available aortic peak velocity data and 31 had available MPA peak velocity data.

Two-dimensional phase-contrast flow quantification versus 4-D flow quantification

Figure 2 summarizes the results of flow quantification based on 2-D phase-contrast MRI compared to 4-D flow-based calculation of net flow, peak systolic velocity and regurgitant fraction. Peak systolic velocities were significantly underestimated by 2-D phase-contrast MRI compared to 4-D flow volumetric analysis for the aorta ($P<0.001$) and the MPA ($P<0.001$) but were not significantly different for the RPA and LPA. Significant differences between 2-D phase-contrast MRI and planar 4-D flow analyses were also found for net flow in the LPA ($P=0.003$) and aorta ($P<0.001$) and LPA regurgitant fractions ($P<0.001$) (Fig. 2). Flow parameters at all other locations were similar for 2-D phase-contrast MRI and 4-D flow.

Velocity assessment by 2-D phase contrast and 4-D flow vs. Doppler echocardiography

Two-dimensional phase-contrast MRI significantly underestimated peak systolic velocity compared to echo in the aorta ($P=0.032$) and MPA ($P<0.001$). In contrast, volumetric flow analysis of 4-D flow resulted in increased (aorta: $P=0.001$) or similar (MPA: $P=0.98$) peak systolic velocities compared to echo. Peak velocity quantification based on volumetric 4-D flow analysis led to significantly increased peak systolic velocities that were underestimated by planar 4-D flow analysis (aorta: $P<0.001$; MPA: $P<0.001$).

Correlation and agreement analysis

Excellent correlation was found between 4-D flow and 2-D phase-contrast MRI for net flow ($r=0.97$, $P<0.001$) and regurgitant fraction ($r=0.87$, $P<0.001$) in the aorta, MPA, RPA and

LPA (Fig. 3). These findings were confirmed by good agreement between 4-D flow and 2-D phase-contrast MRI for net flow (Figs. 3 and 4) as indicated by minimal mean difference and low limits of agreement. Good correlation (r=0.88, P<0.001) was also found between 4-D flow and 2-D phase-contrast MRI for aortic, MPA, RPA and LPA regurgitant fractions (Fig. 3). However the Bland-Altman analysis shows the limits of agreement covering a range of +/−30% between 2-D phase-contrast MRI and 4-D flow for regurgitant fraction assessment (Fig. 4). For peak systolic velocities, a significant but more moderate correlation was found between volumetric 4-D flow and 2-D phase-contrast MRI (r=0.43, P<0.001) and between volumetric 4-D flow and echo (r=0.45, P<0.001) (Fig. 3), indicating differences between volumetric 4-D flow analysis and planar 2-D phase contrast MRI and echo. Bland-Altman analysis confirmed moderate agreement for peak systolic velocities between volumetric 4-D flow and planar 2-D phase-contrast MRI and between volumetric 4-D flow and echo (Fig. 4). Mean differences of 0.2 m/s and 0.3 m/s between 4-D flow volumetric analyses and 2-D phase contrast MRI or echo further indicate the potential of 4-D flow to better assess peak systolic velocities (Fig. 4).

Correlation analysis was employed to assess the internal consistency of the total flow measurements, or conservation of mass, by comparing MPA flow to the sum of RPA and LPA flow for any patients who had 2-D phase-contrast MRI in all of these vessels. Fontan patients were excluded from this analysis. Excellent correlation was found for both 2-D phase-contrast MRI (r=0.95) and 4-D flow (r=0.92) between the sum of RPA and LPA flow and MPA flow (Fig. 5).

Discussion

There is good agreement between 2-D phase-contrast MRI and 4-D flow for net flow, regurgitant fractions, and conservation of mass in our population of children and young adults. Nordmeyer et al. [22] compared 2-D phase-contrast MRI with 4-D flow in seven adult volunteers and found good agreement between ascending aortic, MPA, RPA and LPA stroke volumes for each technique. Nordmeyer et al. [23] also compared 2-D phase-contrast MRI and ascending aortic and MPA 4-D flow in 18 adults with aortic and pulmonary valve stenosis and found no significant difference between the two imaging techniques for stroke volumes and regurgitant fractions. In another study, Valverde and colleagues [24] compared 2-D phase-contrast MRI to 4-D flow in 29 children with single-ventricle physiology and showed excellent correlation between flow in the ascending aorta, MPA, RPA and LPA [24]. Hsiao and colleagues [21] found good correlation between 2-D phase-contrast MRI and 4-D flow (ρ=0.90, r^2= 0.82) for ascending aortic and MPA stroke volumes in 29 children referred for cardiac MRI. Although there are no criteria for defining a clinically significant difference in flow parameters between 2-D phase-contrast MRI and 4-D flow, a difference of less than 10% is thought to be reasonable. Our large pediatric study adds to the growing body of evidence suggesting that there is good agreement between 2-D phase-contrast MRI and 4-D-flow-derived flow parameters.

For peak systolic velocity assessment, 2-D phase-contrast MRI significantly underestimated aortic and MPA peak systolic velocities compared to volumetric 4-D flow and echo (Fig. 2). Despite the lower spatial and temporal resolution of 4-D flow, 4-D flow volumetric aortic

peak systolic velocity values were not underestimated and averaged slightly higher than echo. The improved peak systolic velocity assessment of volumetric 4-D flow employed by this study occurred because the volumetric approach has the advantage of being able to assess velocity data within the entire vessel volume of interest. Compared to 2-D phase-contrast MRI and echo, the volumetric peak velocity analysis was thus independent of the manual definition of an analysis plane but included all velocities in the entire vessel segment to automatically detect peak values independent of their location. All velocity data within the volume can be extracted retrospectively to ascertain the peak velocity without having to target the specific 2-D slice containing the peak velocity information as is required for 2-D phase-contrast MRI and the planar 4-D flow peak velocity assessment approaches.

Nordmeyer et al. [23] compared systolic peak velocity obtained by 2-D phase-contrast MRI with 4-D flow in seven adult volunteers, and they compared 2-D phase-contrast MRI with 4-D flow and echo in 18 adults with aortic or pulmonary valve stenosis. Peak systolic velocity was determined at four predefined locations in the ascending aorta and three levels in the MPA. They utilized streamline visualization to locate the maximum systolic velocity and placed a plane at that level for quantification of peak systolic velocity. For their volunteers, no significant difference was seen between the maximum velocity obtained by 2-D phase contrast MRI and 4-D flow in the ascending aorta and MPA ($P>0.05$). For their patients, peak systolic velocities across the ascending aorta and MPA obtained by 4-D flow were significantly higher than at 2-D phase-contrast MRI ($P=0.025$), and peak systolic velocity obtained by echo across the aortic valve was significantly higher than that of 2-D phase-contrast MRI ($P<0.01$) but was not different from that of 4-D flow ($P>0.05$). Similar to the results of our study, targeted 4-D flow resulted in significantly higher systolic peak velocity, and absolute deviation between 2-D phase contrast MRI and echo was larger than the deviation between 4-D flow and echo. Although their targeted predefined velocity assessment technique is slightly different from our volumetric peak velocity assessment approach, both studies show that 4-D flow improves peak velocity assessment relative to 2-D phase-contrast MRI.

Although the acquisition time for 4-D flow is greater than each individual 2-D phase-contrast MRI sequence, the sum of multiple 2-D phase-contrast MRI sequences in a patient with complex congenital heart disease may add up to more time than the single 4-D flow acquisition (Table 1). This makes the 4-D flow technique especially valuable for assessing complex flow in congenital heart disease where many 2-D phase-contrast MRI planes may need to be acquired. Additionally, data manipulation is possible any time after acquisition of the full 4-D flow volume. Four-dimensional flow also gives insight into blood flow hemodynamics by employing the option of blood flow 3-D visualization and the investigation of blood flow patterns and direction [13, 15, 16]. Therefore 4-D flow has the potential to provide the more quantitative and qualitative flow parameter information than multiple 2-D phase-contrast MRI acquisitions.

Low acquired spatial and temporal resolution is a limiting factor of 4-D flow because increasing temporal and spatial resolution must be balanced with acquisition time. This limitation has become less of an issue with the development of the spatio-temporal imaging acceleration techniques k-t BLAST (spatially and temporally accelerated Broad-use Linear

Acquisition Speed-up Technique) or k-t GRAPPA [12, 33], which can be used to increase the spatial resolution of the 4-D flow data while keeping the scan time similar. This is of particular interest in children in whom small vessels and fast circulation times require improved resolution, but issues with sedation and ability to cooperate for long examinations play important roles.

The velocity encoding values for our 2-D phase-contrast MRI and 4-D flow sequences were adjusted to avoid phase data aliasing. We did not use a standard velocity encoding value and this could result in different signal-to-noise and dynamic ranges in each dataset. However, the bias introduced by aliasing and the attempt to correct it would likely introduce more error than the noise and dynamic range variation. This issue may be overcome by using dual velocity encoding approaches, which are under development [34].

Data for this study were acquired using a 4-D flow pulse sequence that only allowed for prospective electrocardiographic (ECG) triggering while 2-D phase-contrast MRI was acquired using retrospective ECG gating allowing for data acquisition during the entire cardiac cycle. Nevertheless, we speculate that there would only be a minor impact on the measured flow parameters such as peak systolic velocity or net flow because flow velocities are typically very low during the last 10–20% of the cardiac cycle that is missed by prospective gating. This is supported by the excellent correlation between 2-D phase-contrast MRI and 4-D flow for net flow (r=0.97) and regurgitant fraction (r=0.88). There may be a greater impact on assessment of regurgitant fraction as a result of prospective ECG triggering, which truncates data acquisition in late diastole and likely contributes to the lower Bland-Altman agreement rate, with the limits of agreement covering a range of +/−30% between 2-D phase-contrast MRI and 4-D flow for regurgitant fraction assessment.

Another limitation of our study is related to the use of different imaging acceleration techniques (k-t GRAPPA compared to standard parallel imaging) for 4-D flow acquisitions in three patients. However, we have recently demonstrated that k-t GRAPPA accelerated 4-D flow data acquisition can be performed with similar image quality and flow visualization and quantification accuracy compared to standard 4-D flow methods [12].

Although the 2-D phase-contrast MRI and 4-D flow acquisitions were performed during the same examination, mean time between MRI and echo was 3.15 months. Some patients were placed under general anesthesia for MRI but not for echo. Anesthetic agents have been shown to cause a dose-dependent decrease in cardiac function, so exact comparison of cardiovascular flow parameters between all patients may not be completely accurate [35].

Conclusion

Four-dimensional flow provides excellent flow parameter results compared to 2-D phase-contrast MRI. In addition, compared to the echo gold standard, 4-D volumetric peak velocity analysis better estimates peak systolic velocity relative to 2-D phase-contrast MRI. Four-dimensional flow has potential to become a clinical alternative to 2-D phase-contrast MRI in children and young adults.

Acknowledgments

Grant support was provided by the National Institutes of Health NHLBI R01HL115828; DFG (Deutsche Forschungsgemeinschaft/German Research Foundation) SCHN-1170/2-1 and SIR (Society of Interventional Radiology) Foundation Pilot Research Grant. The funding organizations did not participate in study design, did not participate in data collection or interpretation, did not help in manuscript writing, and did not participate in the manuscript submission decision.

The authors wish to thank Marci Messina, RT(R)(MR), for her assistance with patient scanning, and Samantha E. Schoeneman, BA, for her assistance with data collection.

References

1. Atkinson DJ, Edelman RR. Cineangiography of the heart in a single breath hold with a segmented turboFLASH sequence. Radiology. 1991; 178:357–360. [PubMed: 1987592]
2. Beerbaum P, Korperich H, Barth P, et al. Noninvasive quantification of left-to-right shunt in pediatric patients: phase-contrast cine magnetic resonance imaging compared with invasive oximetry. Circulation. 2001; 103:2476–2482. [PubMed: 11369688]
3. Chai P, Mohiaddin R. How we perform cardiovascular magnetic resonance flow assessment using phase-contrast velocity mapping. J Cardiovasc Magn Reson. 2005; 7:705–716. [PubMed: 16136862]
4. Didier D. Assessment of valve disease: qualitative and quantitative. Magn Reson Imaging Clin N Am. 2003; 11:115–134. [PubMed: 12797514]
5. Gatehouse PD, Keegan J, Crowe LA, et al. Applications of phase-contrast flow and velocity imaging in cardiovascular MRI. Eur Radiol. 2005; 15:2172–2184. [PubMed: 16003509]
6. Pelc NJ, Bernstein MA, Shimakawa A, et al. Encoding strategies for three-direction phase-contrast MR imaging of flow. J Magn Reson Imaging. 1991; 1:405–413. [PubMed: 1790362]
7. Underwood SR, Firmin DN, Klipstein RH, et al. Magnetic resonance velocity mapping: clinical application of a new technique. Br Heart J. 1987; 57:404–412. [PubMed: 3496109]
8. Jung B, Honal M, Ullmann P, et al. Highly k-t-space-accelerated phase-contrast MRI. Magn Reson Med. 2008; 60:1169–1177. [PubMed: 18958854]
9. Uribe S, Beerbaum P, Sorensen TS, et al. Four-dimensional (4D) flow of the whole heart and great vessels using real-time respiratory self-gating. Magn Reson Med. 2009; 62:984–992. [PubMed: 19672940]
10. Hsiao A, Lustig M, Alley MT, et al. Rapid pediatric cardiac assessment of flow and ventricular volume with compressed sensing parallel imaging volumetric cine phase-contrast MRI. AJR Am J Roentgenol. 2012; 198:W250–259. [PubMed: 22358022]
11. Tariq U, Hsiao A, Alley M, et al. Venous and arterial flow quantification are equally accurate and precise with parallel imaging compressed sensing 4D phase contrast MRI. J Magn Reson Imaging. 2013; 37:1419–1426. [PubMed: 23172846]
12. Schnell S, Markl M, Entezari P, et al. k-t GRAPPA accelerated four-dimensional flow MRI in the aorta: effect on scan time, image quality, and quantification of flow and wall shear stress. Magn Reson Med. 2014; 72:522–533. [PubMed: 24006309]
13. Bachler P, Valverde I, Pinochet N, et al. Caval blood flow distribution in patients with Fontan circulation: quantification by using particle traces from 4D flow MR imaging. Radiology. 2013; 267:67–75. [PubMed: 23297331]
14. Francois CJ, Srinivasan S, Schiebler ML, et al. 4D cardiovascular magnetic resonance velocity mapping of alterations of right heart flow patterns and main pulmonary artery hemodynamics in tetralogy of Fallot. J Cardiovasc Magn Reson. 2012; 14:16. [PubMed: 22313680]
15. Frydrychowicz A, Markl M, Hirtler D, et al. Aortic hemodynamics in patients with and without repair of aortic coarctation: in vivo analysis by 4D flow-sensitive magnetic resonance imaging. Invest Radiol. 2011; 46:317–325. [PubMed: 21285892]
16. Geiger J, Hirtler D, Burk J, et al. Postoperative pulmonary and aortic 3D haemodynamics in patients after repair of transposition of the great arteries. Eur Radiol. 2014; 24:200–208. [PubMed: 23995974]

17. Geiger J, Markl M, Jung B, et al. 4D-MR flow analysis in patients after repair for tetralogy of Fallot. Eur Radiol. 2011; 21:1651–1657. [PubMed: 21720942]
18. Markl M, Geiger J, Jung B, et al. Noninvasive evaluation of 3D hemodynamics in a complex case of single ventricle physiology. J Magn Reson Imaging. 2012; 35:933–937. [PubMed: 22271353]
19. Uribe S, Bachler P, Valverde I, et al. Hemodynamic assessment in patients with one-and-a-half ventricle repair revealed by four-dimensional flow magnetic resonance imaging. Pediatr Cardiol. 2013; 34:447–451. [PubMed: 22447380]
20. Valverde I, Simpson J, Schaeffter T, et al. 4D phase-contrast flow cardiovascular magnetic resonance: comprehensive quantification and visualization of flow dynamics in atrial septal defect and partial anomalous pulmonary venous return. Pediatr Cardiol. 2010; 31:1244–1248. [PubMed: 20848278]
21. Hsiao A, Alley MT, Massaband P, et al. Improved cardiovascular flow quantification with time-resolved volumetric phase-contrast MRI. Pediatr Radiol. 2011; 41:711–720. [PubMed: 21221566]
22. Nordmeyer S, Riesenkampff E, Crelier G, et al. Flow-sensitive four-dimensional cine magnetic resonance imaging for offline blood flow quantification in multiple vessels: a validation study. J Magn Reson Imaging. 2010; 32:677–683. [PubMed: 20815066]
23. Nordmeyer S, Riesenkampff E, Messroghli D, et al. Four-dimensional velocity-encoded magnetic resonance imaging improves blood flow quantification in patients with complex accelerated flow. J Magn Reson Imaging. 2013; 37:208–216. [PubMed: 22976284]
24. Valverde I, Nordmeyer S, Uribe S, et al. Systemic-to-pulmonary collateral flow in patients with palliated univentricular heart physiology: measurement using cardiovascular magnetic resonance 4D velocity acquisition. J Cardiovasc Magn Reson. 2012; 14:25. [PubMed: 22541134]
25. Barker AJ, Roldan-Alzate A, Entezari P, et al. Four-dimensional flow assessment of pulmonary artery flow and wall shear stress in adult pulmonary arterial hypertension: results from two institutions. Magn Reson Med. 2014 Epub ahead of print. 10.1002/mrm.25326
26. Markl M, Wallis W, Harloff A. Reproducibility of flow and wall shear stress analysis using flow-sensitive four-dimensional MRI. J Magn Reson Imaging. 2011; 33:988–994. [PubMed: 21448968]
27. Markl M, Wegent F, Zech T, et al. In vivo wall shear stress distribution in the carotid artery: effect of bifurcation geometry, internal carotid artery stenosis, and recanalization therapy. Circ Cardiovasc Imaging. 2010; 3:647–655. [PubMed: 20847189]
28. Stankovic Z, Jung B, Collins J, et al. Reproducibility study of four-dimensional flow MRI of arterial and portal venous liver hemodynamics: influence of spatio-temporal resolution. Magn Reson Med. 2014; 72:477–484. [PubMed: 24018798]
29. Bock J, Frydrychowicz A, Stalder AF, et al. 4D phase contrast MRI at 3 T: effect of standard and blood-pool contrast agents on SNR, PC-MRA, and blood flow visualization. Magn Reson Med. 2010; 63:330–338. [PubMed: 20024953]
30. Markl M, Harloff A, Bley TA, et al. Time-resolved 3D MR velocity mapping at 3 T: improved navigator-gated assessment of vascular anatomy and blood flow. J Magn Reson Imaging. 2007; 25:824–831. [PubMed: 17345635]
31. Walker PG, Cranney GB, Scheidegger MB, et al. Semiautomated method for noise reduction and background phase error correction in MR phase velocity data. J Magn Reson Imaging. 1993; 3:521–530. [PubMed: 8324312]
32. Bock, J.; Kreher, BW.; Hennig, J.; Markl, M. Optimized preprocessing of time-resolved 2D and 3D phase contrast MRI data. Proceedings of the 15th annual meeting ISMRM; Berlin, Germany. 2007. p. 3138
33. Jung B, Ullmann P, Honal M, et al. Parallel MRI with extended and averaged GRAPPA kernels (PEAK-GRAPPA): optimized spatiotemporal dynamic imaging. J Magn Reson Imaging. 2008; 28:1226–1232. [PubMed: 18972331]
34. Nett EJ, Johnson KM, Frydrychowicz A, et al. Four-dimensional phase contrast MRI with accelerated dual velocity encoding. J Magn Reson Imaging. 2012; 35:1462–1471. [PubMed: 22282344]
35. De Hert SG. Volatile anesthetics and cardiac function. Semin Cardiothorac Vasc Anesth. 2006; 10:33–42. [PubMed: 16703232]

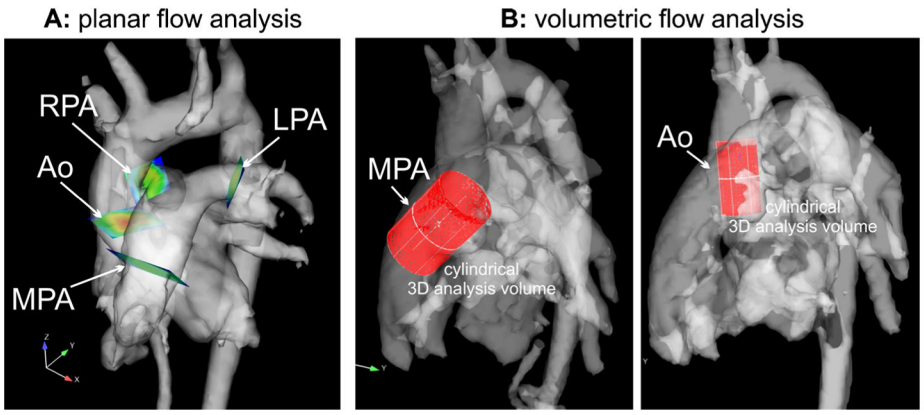

Fig. 1.

Retrospective flow quantification using 4-D flow reconstructed 3-D phase-contrast MR angiography data. **a** Location of analysis planes in the aorta and pulmonary system used for planar flow quantification. Four 2-D analysis planes were manually positioned in the aortic and pulmonary systems. **b** Volumetric analysis for the identification of peak blood flow velocities in the aorta and MPA. *Ao* aortic root (**a**), *Ao* aortic root/ascending aorta (**b**), *MPA* main pulmonary artery, *RPA/LPA* right/left pulmonary arteries

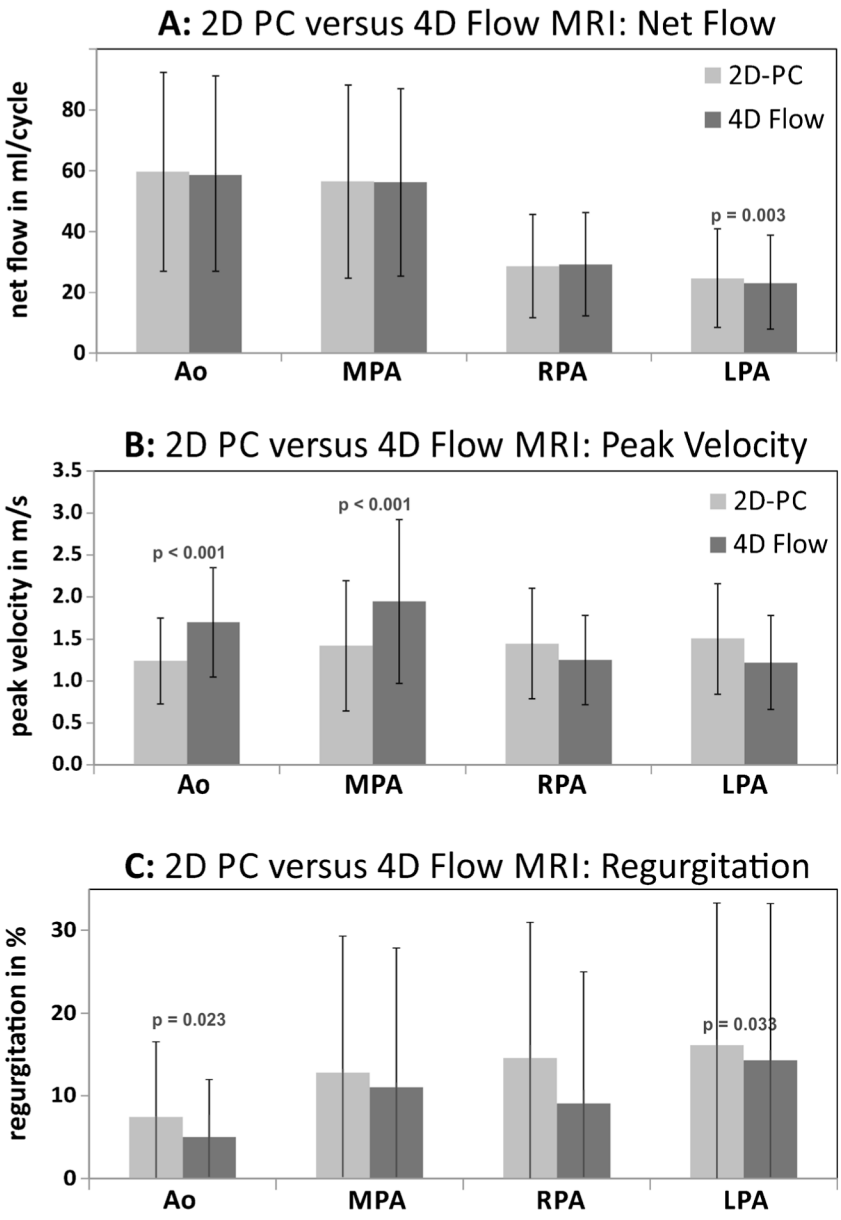

Fig. 2.

Graphs show comparison of aortic and pulmonary flow parameters between 2-D phase-contrast (PC) MRI and quantification based on 4-D flow. Comparisons are for (**a**) net flow, (**b**) peak systolic velocity and (**c**) regurgitant fraction. Volumetric flow analysis (Fig. 1) in the aortic root/ascending aorta was used for 4-D flow-based peak systolic velocity quantification (**b**) in the aortic root/ascending aorta and MPA. *Ao* aorta, *LPA* left pulmonary artery, *MPA* main pulmonary artery, *RPA* right pulmonary artery

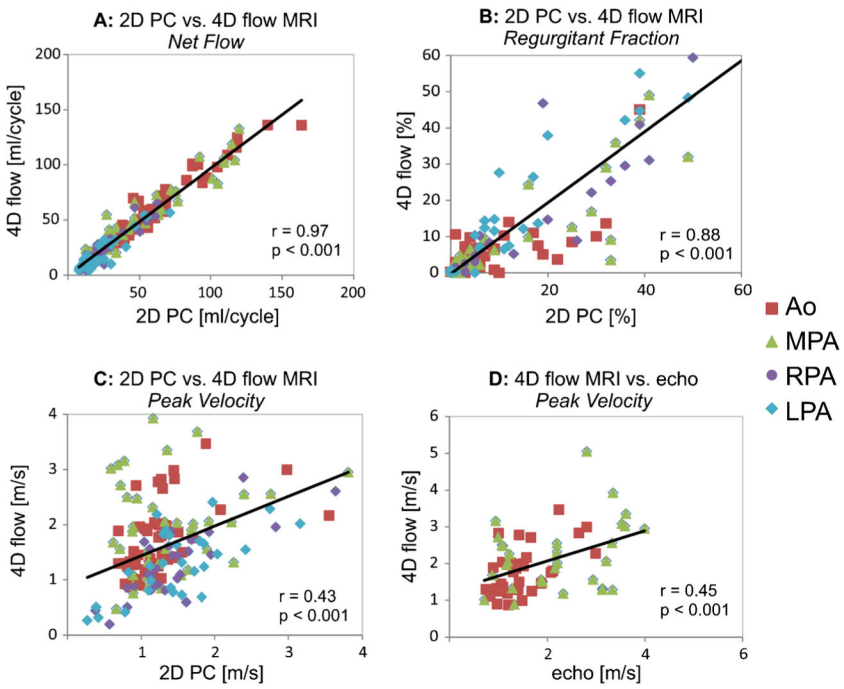

Fig. 3.

Graphs show correlation of aortic and pulmonary flow parameters between 4-D flow and 2-D phase-contrast (PC) MRI. Correlations are for net flow (**a**), regurgitant fraction (**b**) and peak systolic velocities (**c**). In addition, correlation analysis was performed for peak systolic velocities obtained by echo and 4-D flow (**d**). **c, d** Volumetric 4-D flow analysis was based on peak systolic velocities in the aortic root/ascending aorta and MPA. *Ao* aorta, *LPA* left pulmonary artery, *MPA* main pulmonary artery, *RPA* right pulmonary artery

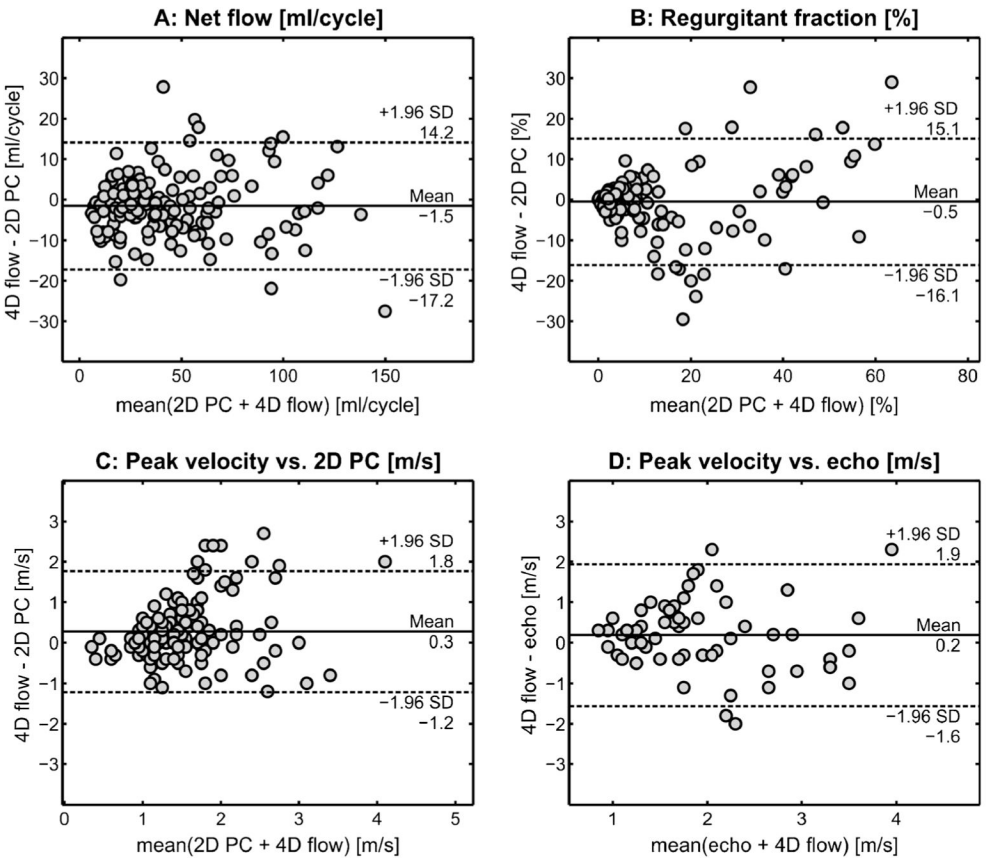

Fig. 4.

Lines of equality and 95% limits of agreement of aortic and pulmonary flow parameters. Bland-Altman plots show the lines of equality between and 95% limits of agreement between 2-D phase-contrast (PC) MRI and 4-D flow for net flow (**a**) and regurgitant fraction in the aorta, MPA, RPA and LPA (**b**), 2-D phase-contrast MRI planar and 4-D flow volumetric peak systolic velocities for the aorta and MPA (**c**), and peak systolic velocities obtained by echo and volumetric 4-D flow in the aorta and MPA (**d**). *LPA* left pulmonary artery, *MPA* main pulmonary artery, *RPA* right pulmonary artery

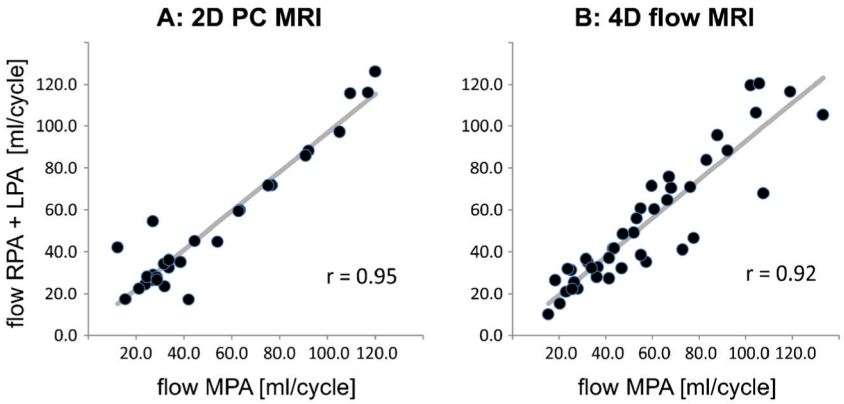

Fig. 5.

Conservation of mass assessment for 2-D phase-contrast (PC) MRI and 4-D flow MRI. Plots assess conservation of mass (sum of flow through LPA and RPAvs. flow through MPA) for 2-D phase-contrast MRI (**a**) and 4-D flow (**b**). *LPA* left pulmonary artery, *MPA* main pulmonary artery, *RPA* right pulmonary artery

Table 1

Pulse sequence acquisition parameters for 2-D phase-contrast MRI and 4-D flow MRI

Sequence parameter	2-D phase-contrast MRI				4-D flow
	Ao	MPA	RPA	LPA	
Temp. resolution (ms)	24.3–56.1	24.0–56.1	21.6–56.5	24.3–55.9	36.8–40.0
TR (ms)	5.7–5.8	5.7–5.8	5.7–5.8	5.7–5.8	4.6–5.0
TE (ms)	2.1–4.4	2.1–4.4	2.1–4.4	2.1–4.3	2.3–2.5
Flip angle (°)	15–20				15
VENC (cm/s)	150–400	150–400	200–400	200–400	100–250
Respiratory motion	Free breathing				Free breathing-navigator
Cardiac gating	Retrospective				Prospective
Reconstructed cardiac time frames	30				9–24
Number of slices	1				22–52
Field of view (mm)	149–308	170–309	149–350	149–340	128–112
	x	x	x	x	x
	199–340	210–340	199–350	199–340	300–400
Phase encoding steps	172–232	172–336	176–360	188–360	68–96
Bandwidth (Hz/pixel)	480–511	480–511	488–491	480–511	445–460
Spatial resolution (mm)	1.0–1.9	1.0–1.9	1.0–1.6	1.0–1.8	2.7–4.1
	x	x	x	x	x
	1.0–1.9	1.0–1.9	1.0–1.6	1.0–1.8	2.0–2.7
Slice thickness (mm)	5–6				2.0–3.5
Signal averages	2–3				1
Acquisition time* (minutes) and acceleration factor (R)	5.86±3.19 (R=2)				R=2: 12.6±5.1 R=5: 6.6±3.0

Ao aortic root, *LPA* left pulmonary artery, *MPA* main pulmonary artery, *R* acceleration factor, *RPA* right pulmonary artery, *TE* echo time, *TR* repetition time, *VENC* velocity encoding

*Listed mean (+/−SD) acquisition time for 2-D phase-contrast MRI represents the mean sum time of all 2-D phase-contrast MRI flow sequences performed per patient

Table 2

Patient characteristics

	Number of patients	Mean age (age range), years
TOF s/p repair	10	10.3 (3.9–14.1)
TGA s/p arterial switch	7	10.8 (5.4–29)
Congenitally corrected TGA	1	29
Ross procedure	4	23.8 (19–28)
Aortic coarctation	4	12.1 (7.1–15.6)
ASD and/or VSD	4	15.5 (10–16)
Bicuspid aortic valve	3	10.5 (4.4–18)
Aortic stenosis (supravalvar, subaortic stenosis)	4	15.8 (6.4–26)
Pulmonary atresia	2	9.7 (9.4–10)
Ventricular ectopy	1	10.5
Left SVC to dilated coronary sinus	1	5.4
Truncus arteriosus s/p repair	1	10.3
Normal	1	15.5
RV dilation, pulmonary regurgitation	1	6.4
Fontan	2	20.4 (20–20.8)
Dilated aortic root	1	10
Dilated LV, RV	1	19
Marfan syndrome s/p aortic root replacement	1	17.4
Pulmonary stenosis s/p valvuloplasty	1	12
Ebstein anomaly	1	9

ASD atrial septal defect, *LV* left ventricle, RV right ventricle, *s/p* status post, *SVC* superior vena cava, *TGA* D-transposition of the great arteries, *TOF* tetralogy of Fallot, *VSD* ventricular septal defect